# Supplementary Data

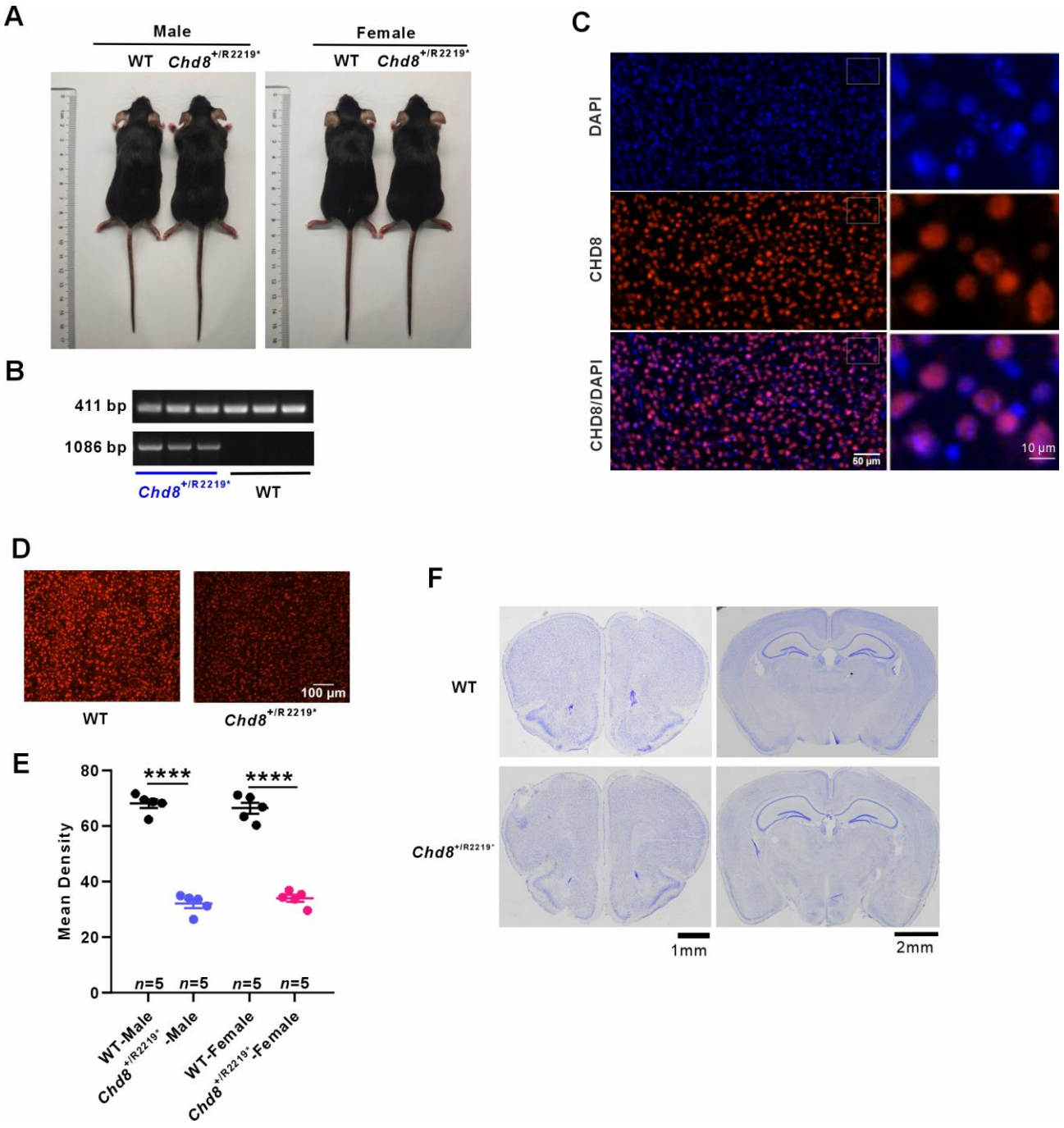


**Fig. S1** Validation data of germline mutant *Chd8*$^{+/R2219*}$ mice, related to Fig. 1. **A** Representative photos of adult *Chd8*$^{+/R2219*}$ and WT mice. **B** Genotype identification by agarose gel electrophoresis of PCR products. **C–E** Decreased expression of Chd8 protein in adult *Chd8*$^{+/R2219*}$ cortex. The red puncta indicate Chd8-expressing neurons (**C, D**), statistical graph of Chd8 expression (**E**), Scale bars, 50 μm, 10 μm, 100 μm. ($n$ = 5, 5, 5, 5, $^{**}P < 0.01$, one-way ANOVA). **F** Representative coronal sections of adult WT and mutant brains with Nissl stain. Scale bars, 1 mm, 2 mm.

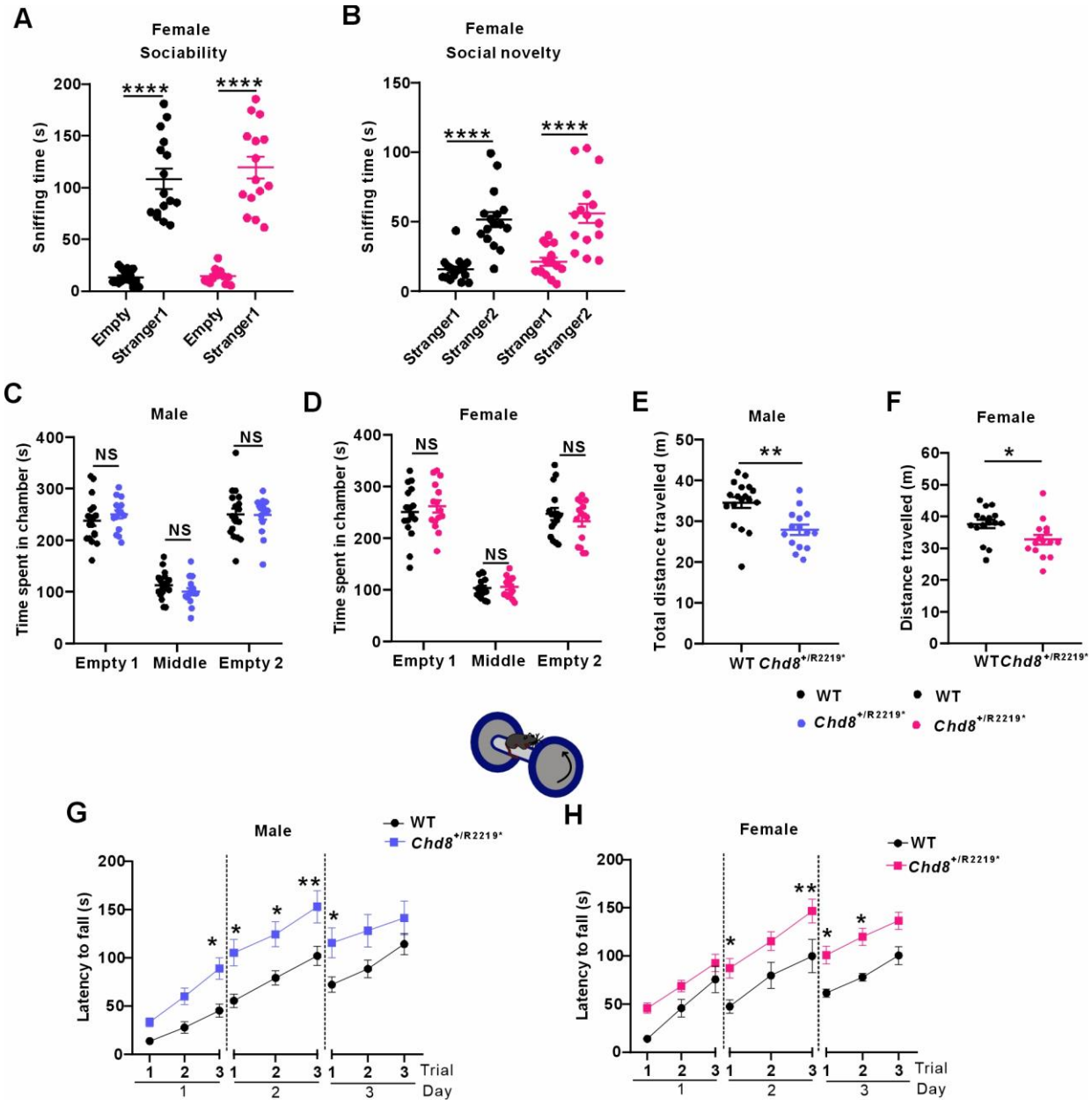


**Fig. S2** Behavioral tests in *Chd8*$^{+/R2219*}$ mice, related to Fig. 2. **A, B** No difference between the two female genotypes in the three-chamber social test. Sniffing time of female mice during (**A**) sociability and (**B**) social novelty stages in the three-chamber test (****$P$ < 0.0001, one-way ANOVA; $n$ = 16, 15). **C, D** Time spent in each chamber during the habituation phase in (**C**) male and (**D**) female mice ($n$ = 18, 15 males and 16, 15 females). **E, F** Reduced total locomotion during the habituation phase for (**E**) male and (**F**) female mice (**$P$ < 0.01, *$P$ < 0.05, unpaired $t$-test; $n$ = 18, 15 males and 16, 15 females). **G, H** Enhanced motor performance of *Chd8*$^{+/R2219*}$ mice on the rotarod. *Chd8*$^{+/R2219*}$ mice exhibited a longer latency to fall than WT in both (**G**) male and (**H**) female groups (mean ± SEM; two-way ANOVA; *$P$ < 0.05, **$P$ < 0.01, NS, not significant; $n$ = 18, 15 males and 16, 15 females). Mice were tested over three consecutive days with three trials per day.

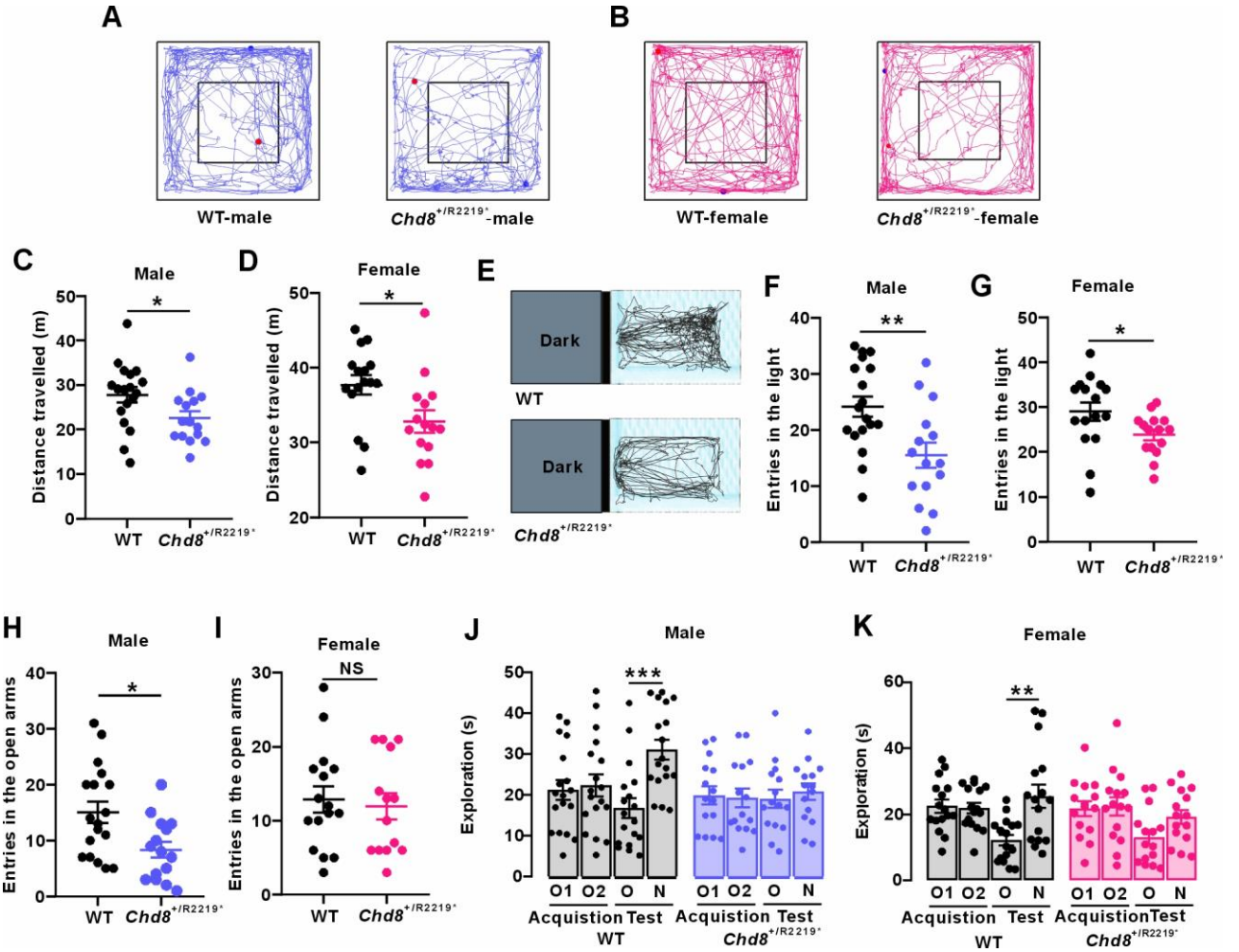


**Fig. S3** Behavioral tests in *Chd8*$^{+/R2219*}$ mice, related to Fig. 3. **A–D** Reduced locomotion of *Chd8*$^{+/R2219*}$ mice in the open field test. (**A**) and (**B**) show representative locomotion traces of *Chd8*$^{+/R2219*}$ and WT mice. (**C**) and (**D**) quantify the total distance traveled (mean ± SEM; **P* < 0.05, unpaired *t*-test; *n* = 18, 15 males and 16,15 females). **E–G** Fewer entries of *Chd8*$^{+/R2219*}$ mice to the light chamber in light-dark test performance. (**E**) Representative movement traces of *Chd8*$^{+/R2219*}$ and WT mice in the light chamber. The number of entries into the light chamber was quantified for (**F**) male and (**G**) female mice (mean ± SEM, unpaired *t*-test; **P* < 0.05, ***P* < 0.01; *n* =18, 15 males and 16, 15 females). **H, I** (**H**) Fewer entries of male, but not (**I**) female, *Chd8*$^{+/R2219*}$ mice to open arms in the elevated plus-maze test (mean ± SEM, unpaired *t*-test; **P* < 0.05; *n* = 18, 15 males and 16, 14 females). **J, K** Reduced sniffing time on novel objects in the novel object recognition test. Sniffing time was quantified for (**J**) male and (**K**) female mice (mean ± SEM; ****P* < 0.0001, one-way ANOVA; NS, not significant; *n* = 18, 15 males and 16, 15 females). O1: object 1; O2: object2; O: old object; N: novel object.

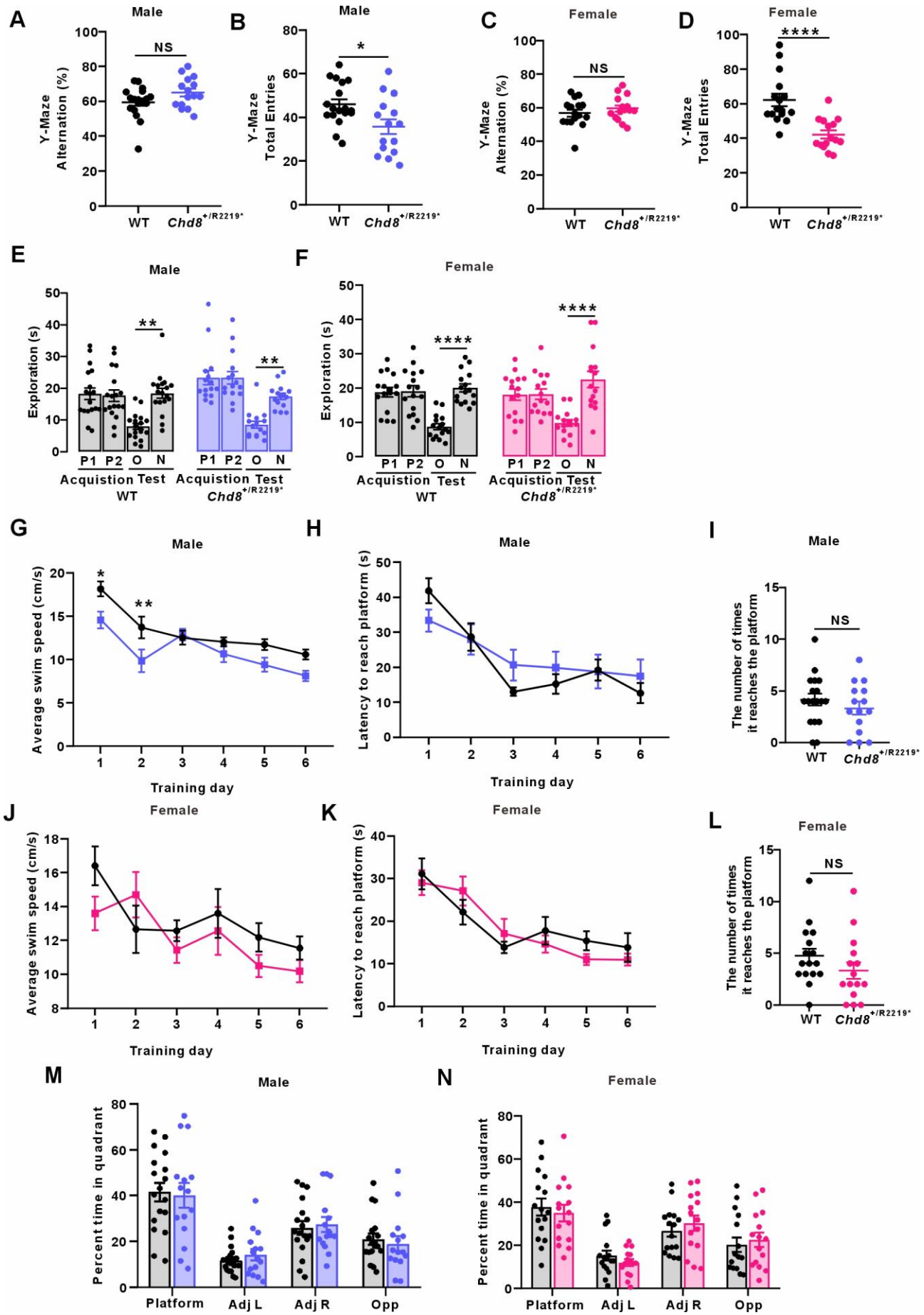
A
Male
Y-Maze Alternation (%)
NS
WT
Chd8+/R2219*
B
Male
Y-Maze Total Entries
*
WT
Chd8+/R2219*
C
Female
Y-Maze Alternation (%)
NS
WT
Chd8+/R2219*
D
Female
Y-Maze Total Entries
****
WT
Chd8+/R2219*
E
Male
Exploration (s)
**
**
P1 P2 O N
Acquistion Test
WT
Chd8+/R2219*
F
Female
Exploration (s)
****
****
P1 P2 O N
Acquistion Test
WT
Chd8+/R2219*
G
Male
Average swim speed (cm/s)
*
**
Training day
H
Male
Latency to reach platform (s)
Training day
I
Male
The number of times it reaches the platform
NS
WT
Chd8+/R2219*
J
Female
Average swim speed (cm/s)
Training day
K
Female
Latency to reach platform (s)
Training day
L
Female
The number of times it reaches the platform
NS
WT
Chd8+/R2219*
M
Male
Percent time in quadrant
Platform
Adj L
Adj R
Opp
N
Female
Percent time in quadrant
Platform
Adj L
Adj R
Opp

**Fig. S4** *Chd8*$^{+/R2219*}$ mice showed normal spatial learning and memory, related to Fig. 3. **A–D** WT and *Chd8*$^{+/R2219*}$ mice showed comparable alternation and decreased total number of entries in the Y-maze test for (**A, B**) male and (**C, D**) female. *$P < 0.05$, ****$P < 0.0001$, unpaired *t*-test; $n = 18$, 15 males and 16, 15 females. **E, F** No difference in novel position recognition between WT and *Chd8*$^{+/R2219*}$ mice. Sniffing time was quantified for old position object and novel position object in (**E**) male and (**F**) female mice (**$P < 0.01$, ****$P < 0.0001$, one-way ANOVA; $n = 18$, 15 males and $n = 16$, 15 females). P1: position 1; P2: position 2; O: old position; N: novel position. **G–N** No difference between WT and *Chd8*$^{+/R2219*}$ mice for both male and female in Morris water maze test. Data represent mean ± SEM; *$P < 0.05$, **$P < 0.01$, two-way ANOVA; NS, not significant; $n = 18$, 15 males and 16, 15 females.

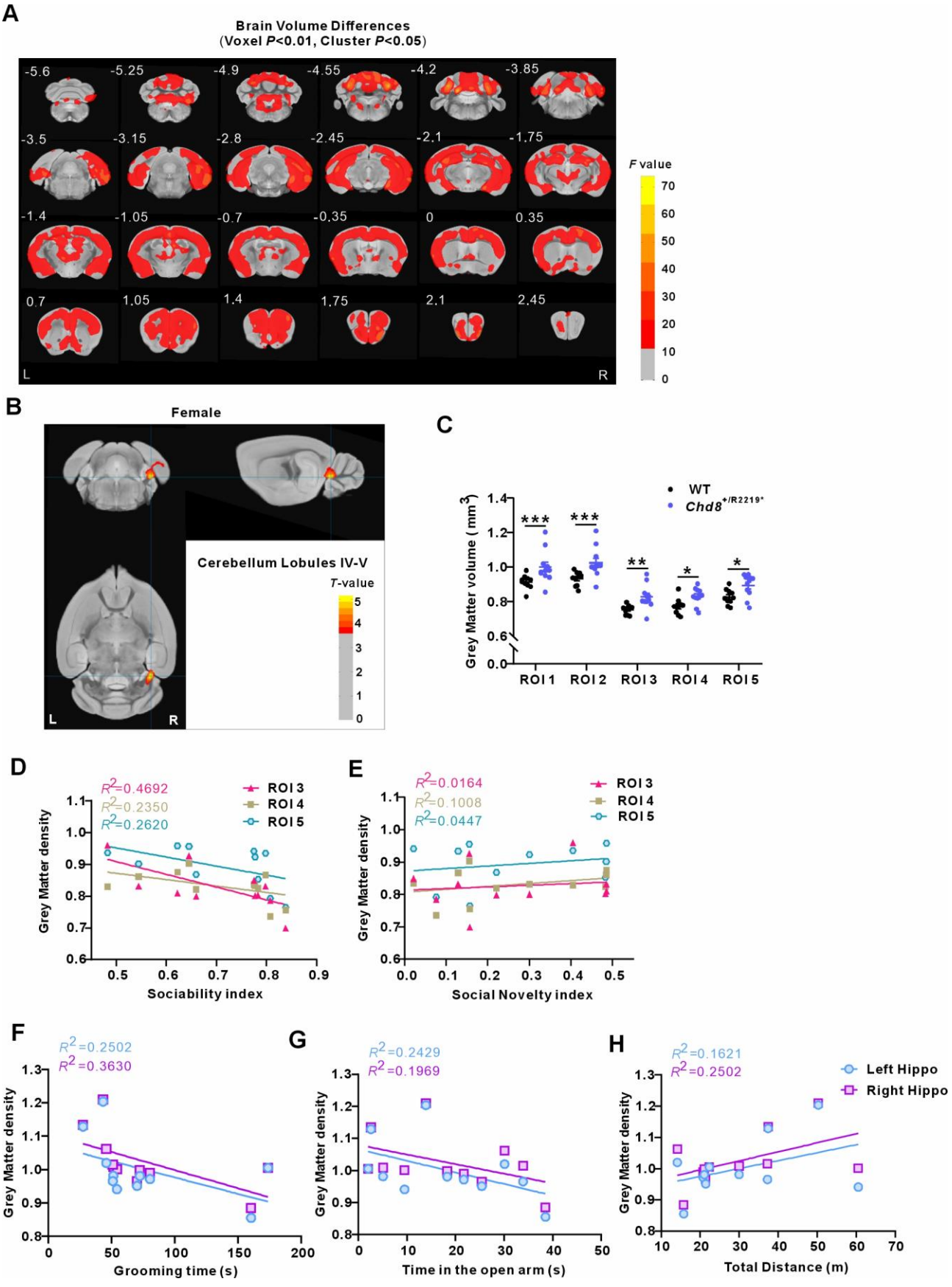


**Fig. S5** Concordance of left or right hippocampal size and other behavior in male *Chd8*$^{+/R2219*}$mice, related to Fig. 4. **A** Voxel-wise differences in volume between *Chd8*$^{+/R2219*}$ and WT littermates, voxel

$P < 0.01$, cluster $P < 0.05$. **B** Female voxel-wise differences in volume (left), quantification of cerebellum lobule VI–V (highlighted with yellow), grey matter volume (right). **C** Quantification of ROI 1–5 grey matter volume. ROIs, highlighted with yellow. ROI 1: left hippocampus, ROI 2: right hippocampus, ROI 3: entorhinal area, ROI 4: simple lobule, ROI 5: declive. ***$P < 0.001$, **$P < 0.01$, *$P < 0.05$, multiple *t*-tests. **D, E** Concordance of grey matter density and sociability (SB, D) ( ROI 3: $P = 0.0200$, ROI 4: $P = 0.1307$, ROI 5: $P = 0.1075$) or social novelty (SN, E) ( ROI 3: $P = 0.7073$, ROI 4: $P = 0.3413$, ROI 5: $P = 0.1075$) difference index in male *Chd8*$^{+/R2219*}$mice. ROI 3: entorhinal area, ROI 4: simple lobule, ROI 5: declive. $n = 11$. **F–H** Concordance of hippocampal grey matter density and grooming time (**F**) (Left Hippo: $P = 0.1172$, Right Hippo: $P = 0.0498$), time in the open arm (**G**) (Left Hippo: $P = 0.1235$, Right Hippo: $P = 0.1716$) or total distance in the open field test (**H**) (Left Hippo: $P = 0.2196$, Right Hippo: $P = 0.1172$). Data represent mean ± SEM.

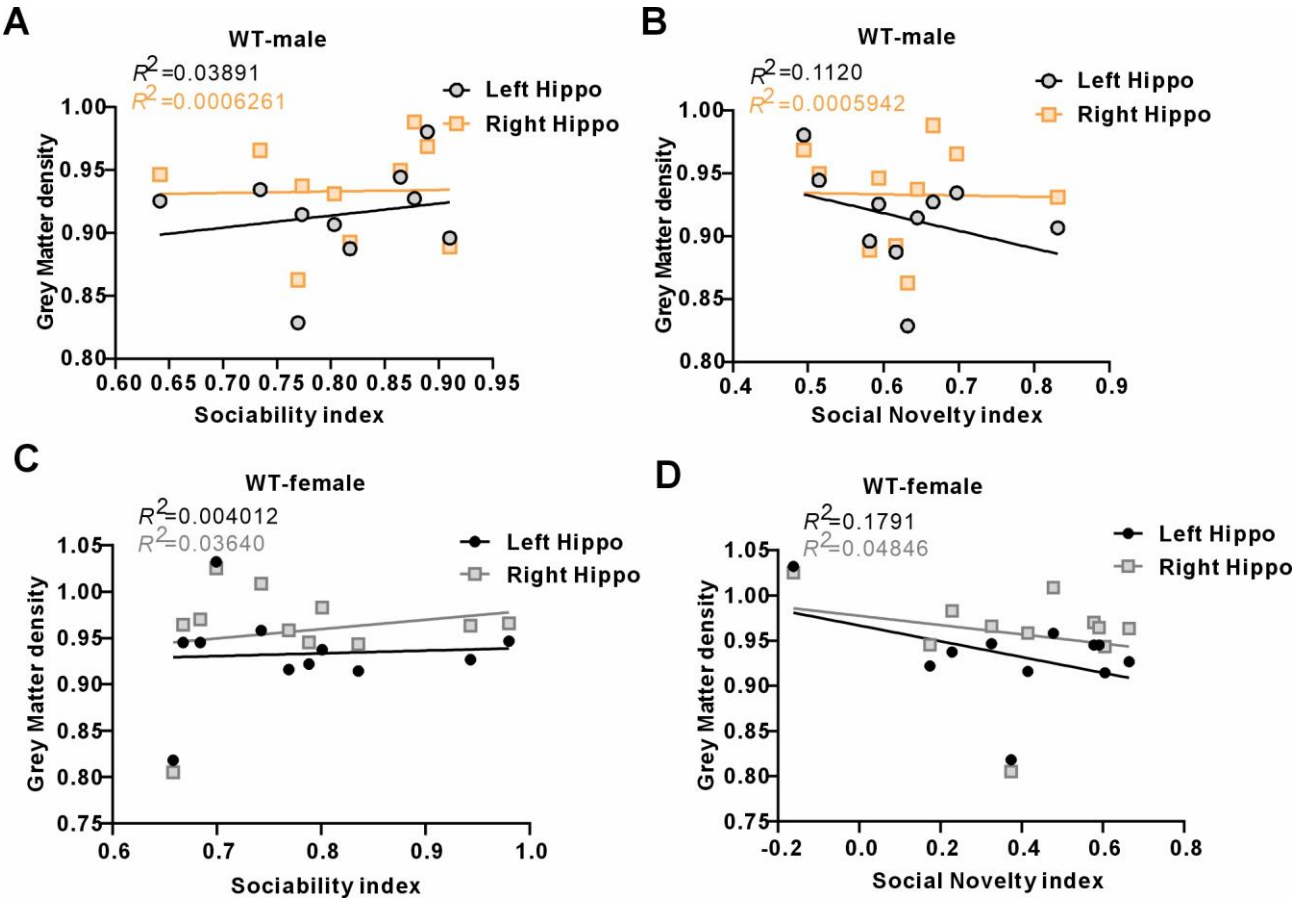


**Fig. S6** Concordance of left or right hippocampal size and social behavior in WT males, related to Fig. 4. **A, B** Concordance of hippocampal grey matter density and sociability (**A**, SB) (Left Hippo: $P = 0.5849$, Right Hippo: $P = 0.9453$) or social novelty (**B**, SN) (Left Hippo: $P = 0.3445$, Right Hippo: $P = 0.9467$) difference index in male WT mice. $n = 10$. **C, D** Concordance of hippocampal grey matter density and sociability (**C**, SB) (Left Hippo: $P = 0.8532$, Right Hippo: $P = 0.5742$) or social

novelty (**D**, SN) (Left Hippo: $P = 0.1946$, Right Hippo: $P = 0.5154$) difference index in female WT mice. $n = 11$.

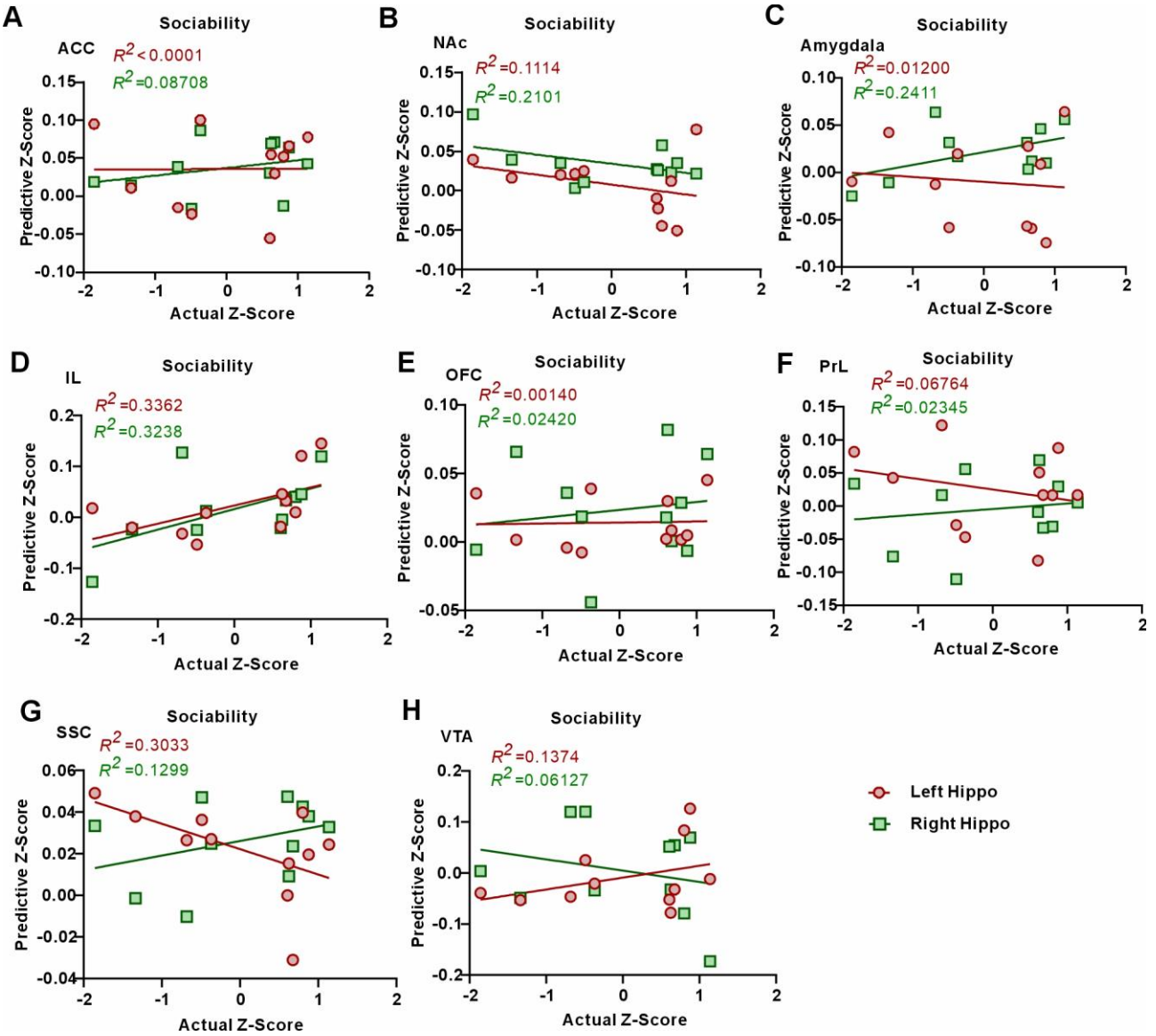


**Fig S7.** The connectivity coefficients between the bilateral hippocampi-seed and a single ROI do not predict sociability. **A–H** Correlation fitting plots of hippocampal-ROI functional connectivity strength vs. Sociability index. Hippocampal-ACC (**A**) (Left Hippo: $P = 0.9848$, Right Hippo: $P = 0.3783$); Hippocampal-NAC (**B**) (Left Hippo: $P = 0.3159$, Right Hippo: $P = 0.1563$); Hippocampal-Amygdala (**C**) (Left Hippo: $P = 0.7485$, Right Hippo: $P = 0.1251$); Hippocampal-IL (**D**) (Left Hippo: $P = 0.0615$, Right Hippo: $P = 0.0677$); Hippocampal-OFC (**E**) (Left Hippo: $P = 0.9129$, Right Hippo: $P = 0.6479$); Hippocampal-PrL (**F**) (Left Hippo: $P = 0.4399$, Right Hippo: $P = 0.6530$); Hippocampal-SSC (**G**) (Left Hippo: $P = 0.0792$, Right Hippo: $P = 0.2763$); Hippocampal-VTA (**H**) (Left Hippo: $P = 0.2617$, Right Hippo: $P = 0.4630$).

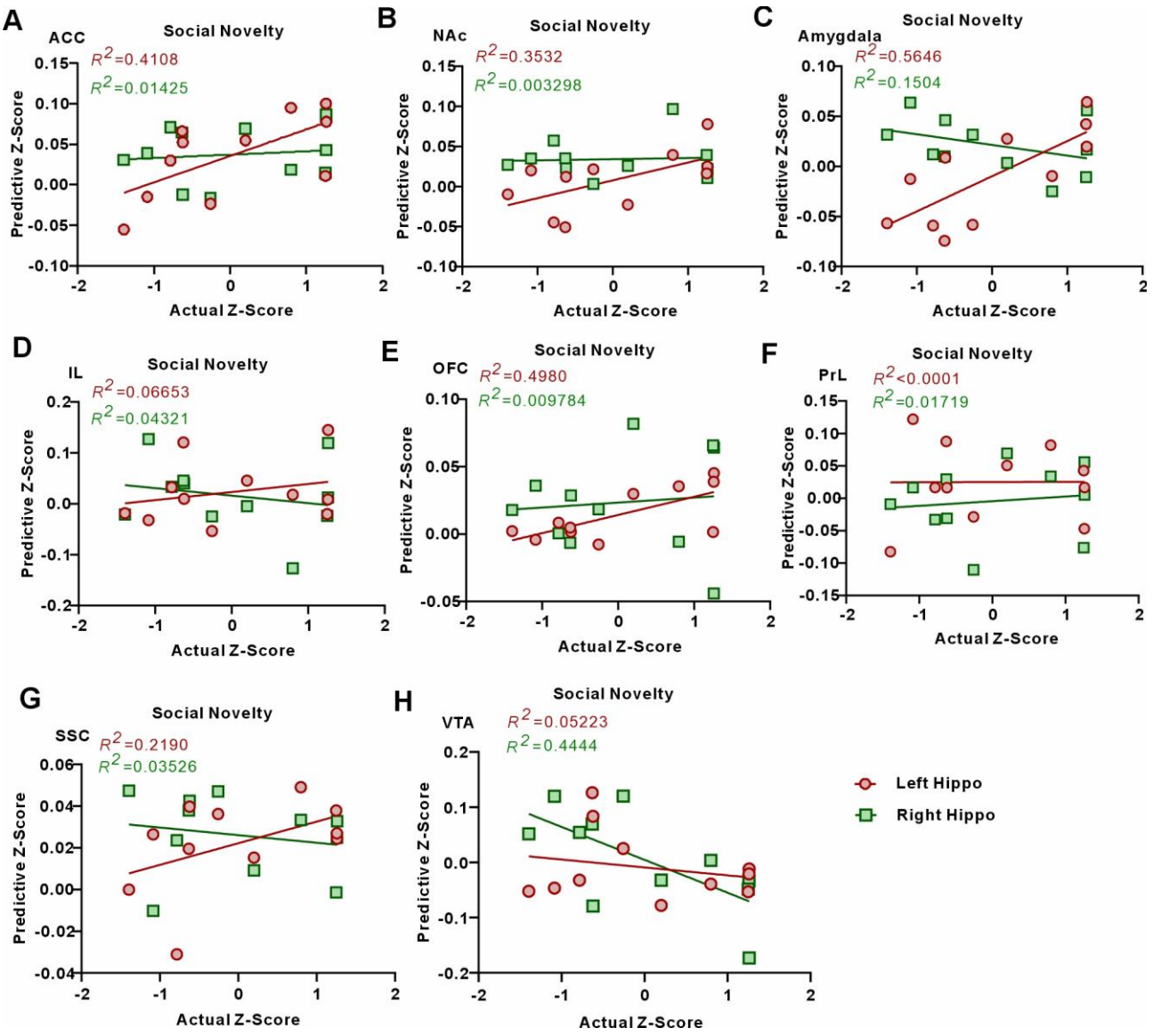


**Fig S8.** The connectivity coefficients between the bilateral hippocampi-seed and a single ROI do not predict social novelty. **A–H** Correlation fitting plots of hippocampal-ROI functional connectivity strength vs. Social novelty index. Hippocampal-ACC (**A**) (Left Hippo: $P = 0.0336$, Right Hippo: $P = 0.7266$); Hippocampal-NAC (**B**) (Left Hippo: $P = 0.0538$, Right Hippo: $P = 0.8668$); Hippocampal-Amygdala (**C**) (Left Hippo: $P = 0.0077$, Right Hippo: $P = 0.2386$); Hippocampal-IL (**D**) (Left Hippo: $P = 0.4438$, Right Hippo: $P = 0.5396$); Hippocampal-OFC (**E**) (Left Hippo: $P = 0.0152$, Right Hippo: $P = 0.7723$); Hippocampal-PrL (**F**) (Left Hippo: $P = 0.9885$, Right Hippo: $P = 0.7008$); Hippocampal-SSC (**G**) (Left Hippo: $P = 0.1466$, Right Hippo: $P = 0.5803$); Hippocampal-VTA (**H**) (Left Hippo: $P = 0.4991$, Right Hippo: $P = 0.0251$).

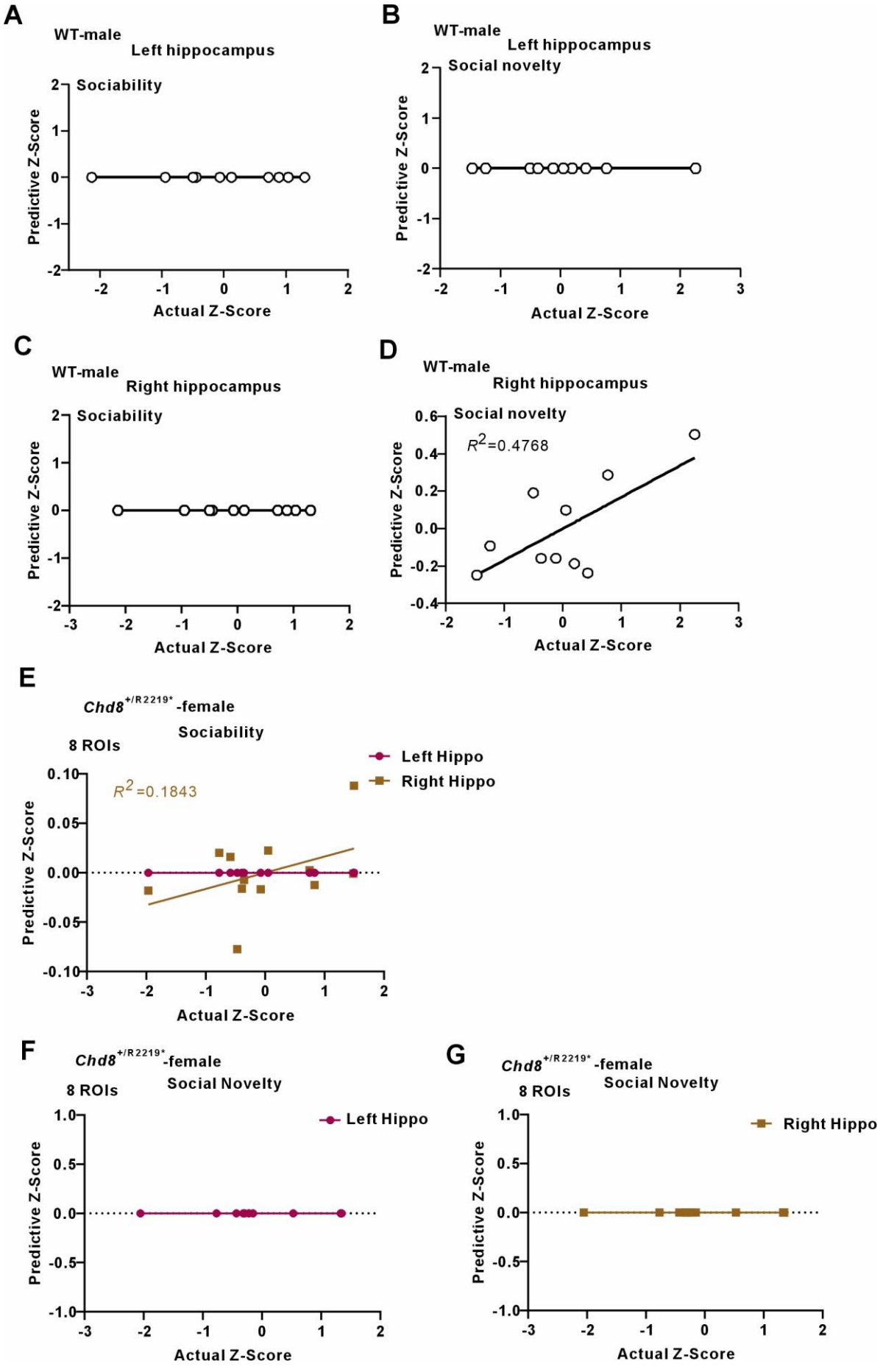
A
WT-male
Left hippocampus
Sociability
Predictive Z-Score
Actual Z-Score
B
WT-male
Left hippocampus
Social novelty
Predictive Z-Score
Actual Z-Score
C
WT-male
Right hippocampus
Sociability
Predictive Z-Score
Actual Z-Score
D
WT-male
Right hippocampus
Social novelty
$R^2$=0.4768
Predictive Z-Score
Actual Z-Score
E
Chd8+/R2219*-female
Sociability
8 ROIs
Left Hippo
Right Hippo
$R^2$=0.1843
Predictive Z-Score
Actual Z-Score
F
Chd8+/R2219*-female
Social Novelty
8 ROIs
Left Hippo
Predictive Z-Score
Actual Z-Score
G
Chd8+/R2219*-female
Social Novelty
8 ROIs
Right Hippo
Predictive Z-Score
Actual Z-Score

**Fig. S9** Integrating coordinated connectivity spectra of all eight ROIs fails to predict social function in WT male mice or female mutants, related to Fig. 5. **A, B** Correlation fitting plots of left hippocampal-ROI functional connectivity strength vs. sociability difference index (**A**) and connectivity strength vs. social novelty difference index (**B**). **C, D** Correlation fitting plots of right hippocampal-ROI functional connectivity strength vs. sociability difference index (**C**) and connectivity strength vs. social novelty difference index (**D**) ($P = 0.0271$). **E** Correlation fitting plots of left or right hippocampal-ROI functional connectivity strength vs. sociability difference index (Right Hippo: $P = 0.1637$). **F** Correlation fitting plots of left hippocampal-ROI functional connectivity strength vs. social novelty difference index. **G** Correlation fitting plots of right hippocampal-ROI functional connectivity strength vs. social novelty difference index.

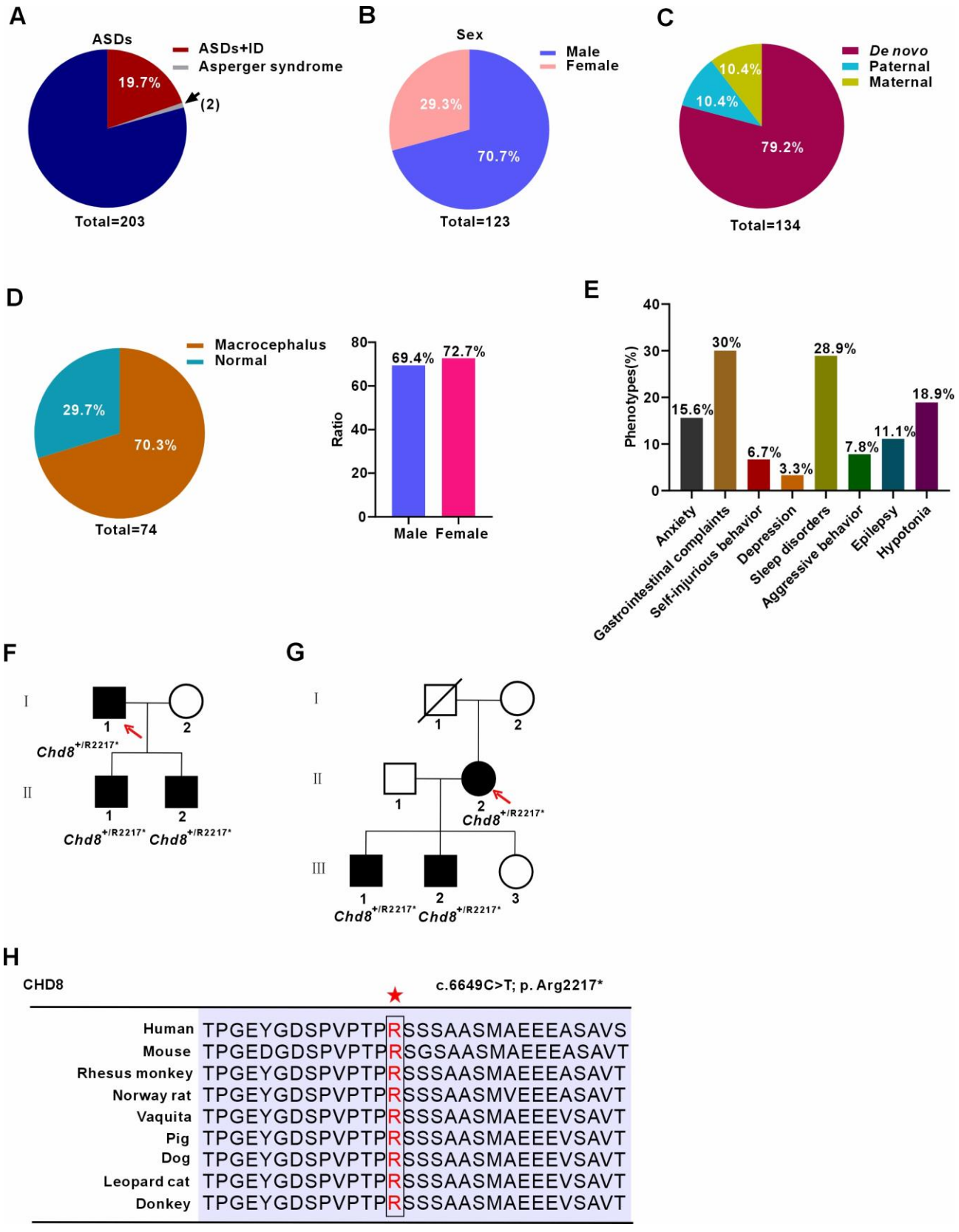


**Fig. S10** Summary of ASDs clinical reports on *CHD8* gene mutations. **A** Pie chart of the proportion of reported diagnostic types of ASDs. **B** Pie chart of the gender distribution proportion. **C** Pie chart of the proportion of reported inheritance of ASDs. **D** Pie chart of the proportion of reported cases

with macrocephaly (left), the proportion of macrocephaly phenotype in male and female patients (right). **E** Concomitant clinical symptoms in patients beyond the core phenotype. **E–G** Pedigree information of patient-derived genetic loci in the model mice constructed in this study, including paternal (**F**) and maternal inheritance patterns (**G**), with the figure adapted from previously reported data. **H** Conservation analysis of amino acid mutation sites across species.